

# The voltage–time behaviour for porous anodizing of aluminium in a fluoride-containing oxalic acid electrolyte

A. Mozalev<sup>a,\*</sup>, A. Poznyak<sup>a</sup>, I. Mozaleva<sup>a</sup>, A.W. Hassel<sup>b</sup>

<sup>a</sup> *Belarusian State University of Informatics and Radioelectronics, 6 Brovka Street, Minsk 220027, Belarus*

<sup>b</sup> *Max-Planck-Institut für Eisenforschung, Max-Planck-Str. 1, 40237 Düsseldorf, Deutschland*

Received 21 February 2001; received in revised form 19 March 2001

## Abstract

A systematic investigation has been undertaken of voltage–time behaviour for galvanostatic porous anodizing of aluminium in 0.4 mol dm<sup>-3</sup> H<sub>2</sub>C<sub>2</sub>O<sub>4</sub> modified by the addition of variable amounts of NH<sub>4</sub>F, in circumstances of varying current density and stirring conditions. Both the concentration of NH<sub>4</sub>F in the electrolyte and stirring of the fluoride-containing (FC) electrolyte appeared to affect the voltage–time response for anodizing aluminium, causing a decrease in the forming voltage. The voltage-reducing effect is further substantially enhanced while the solution is stirred. Despite a tenfold decrease in the anodizing voltage in the FC electrolyte, no apparent changes in pore morphology are determined from SEM observation. The phenomena described are explained by considering formation of FC electrolyte-derived species and their incorporation into growing oxide film. © 2001 Published by Elsevier Science B.V.

**Keywords:** Anodizing; Porous alumina; Voltage–time response; Fluoride species; Incorporation

## 1. Introduction

Anodizing of aluminium is used for producing nanoporous isolating films suitable for diverse applications in electronics and microelectronics, including passivating coatings, thin-film resistors, capacitors, inductors, and planarized interconnections for integrated circuits [1–5]. Practically, porous-type films on aluminium are most simply formed by galvanostatic anodizing in aqueous acidic solutions, using current densities of 6–10 mA cm<sup>-2</sup> at anodic voltages 40–200 V [6]. Recently, anodizing has been employed for forming self-planarized aluminium interconnections for CMOS ULSI with a minimal resolution of 1.2 μm [7]. Considering most recent achievements in submicron ULSI technology [8], future progress in application of anodizing technique is associated with a substantial reducing the anodizing voltage at appropriate current densities and room temperature to form a self-planarizing dielectric incorporated in array of super-narrow metal lines. Anodizing at relatively low voltages (15–25 V) is possible in sulphuric

acid solutions [9]; however, high aggressiveness of such electrolytes has made their utilization very problematic. Although it was mentioned in previous work that aluminium anodizing was performed in an oxalic acid-based electrolyte at 10–30 V, neither the electrolyte content nor the anodizing variables were reported [7]. The development of a low-voltage anodizing process is expected to reliably protect the active part of a CMOS ULSI (especially, gate isolator), to allow thinning of protecting masks and underlayers, and to achieve submicron metal/oxide resolution. Besides, as it is generally believed that the forming voltage largely decides pore morphology [10], porous alumina films formed at low voltages are of considerable interest as models for growth of super fine porous-cellular structure.

One of the approaches to contribute to the double layer charge and, hence, to achieve a substantial voltage change is the modification of anodizing solution by adding a complexing agent, capable of reacting with electrolyte anions and species with further absorbing and incorporating the products formed into growing oxide film. In this work, galvanostatic anodizing of aluminium to form porous oxide was performed and studied in oxalic acid solutions with the addition of variable amounts of ammonium fluoride, in a wide

\* Corresponding author. Tel.: +375-172398047; fax: +375-172310914.

E-mail address: sasha@nys.by (A. Mozalev).

range of current densities and in circumstances of varying stirring conditions.

## 2. Experimental

Initial experimental specimens were prepared by vacuum depositing 99.99% aluminium films, 3  $\mu\text{m}$  thick, onto oxide-coated silicon wafers. The wafers were then cut into pieces of ca.  $3 \times 3 \text{ cm}^2$  and subjected to electrochemical anodizing in a PTFE two-electrode cell filled with an aqueous electrolyte. A tungsten spiral of a large surface area was used as the counter electrode. A PTFE protecting ring, fixed tightly on the aluminium surface, confined the anodizing area within a circle of 1.4 cm diameter. A P5827M potentiostat (Belarus) equipped with a step-up output divider was employed as the anodizing unit. An aqueous  $0.4 \text{ mol dm}^{-3} \text{ H}_2\text{C}_2\text{O}_4$  was used as the working solution, which was then modified by adding variable amounts of  $\text{NH}_4\text{F}$ , in circumstances of varying stirring conditions. Concentration of ammonium fluoride in the working solution was raised up to  $2.5 \text{ mmol dm}^{-3}$ . The aluminium specimens were anodized at a constant current density of  $10\text{--}400 \text{ mA cm}^{-2}$ . Temperature of the electrolyte was kept at 293 K. Voltage value taking up during galvanostatic anodizing of aluminium as a function of anodizing time was automatically registered. Porous-cellular structure of oxide films formed was observed in a Hitachi S-806 scanning electron microscope (SEM).

## 3. Results

### 3.1. Non-stirred electrolyte

A set of the voltage–time curves for anodizing aluminium at  $10 \text{ mA cm}^{-2}$  in the non-stirred fluoride-containing (FC) electrolyte of variable concentrations in  $\text{NH}_4\text{F}$  is shown in Fig. 1(a) and compared with the voltage–time curve for anodizing in the non-stirred fluoride-free (FF) working solution. In case of the FF working solution (curve 1), the forming voltage increases almost linearly up to about 50 V, before reaching a maximum (critical voltage,  $E_{\text{cr}}$ , as pointed out in Fig. 1(a)) of 54 V and then decreases gradually until a steady-state value of 48 V is achieved, which is quite usual for anodizing aluminium in oxalic acid solutions [11]. In the FC electrolyte, the value of  $E_{\text{cr}}$  lowers with increasing  $\text{NH}_4\text{F}$  concentration,  $C_{\text{F}}$ . At the very initial concentrations of ammonium fluoride, the voltage–time behaviour looks rather similar to that in the FF working solution (curves 1–3). Consequently, with further increase in  $C_{\text{F}}$  after the initial voltage rise to a maximum, a relative decrease in voltage occurs, after which the voltage slightly increases again, resulting in a downward cur-

vature in the segment of the curves between 4 and 6 min, where  $E_{\text{cur}}$  is the centre of the curvature (see curves 4–6 in Fig. 1(a)). After 6 min the forming voltage still continues to increase, but linearly and at a rate depending upon  $\text{NH}_4\text{F}$  concentration. The slope  $dE/dt$  of this linear voltage rise becomes obviously greater with increasing  $C_{\text{F}}$ , reaching eventually about  $0.7 \text{ V min}^{-1}$ . The voltage ‘stoop’, which is usual for porous-type film formation [11], becomes smaller and flatter with increasing  $C_{\text{F}}$  (curves 7–8) and, beyond  $2.0 \text{ mmol dm}^{-3}$  the relative voltage decrease vanishes, leaving just a slightly downward curvature on the rising curves 9 and 10. A further feature is that, within 2 min of the initial voltage rise, the voltage elevation retards while the concentration of  $\text{NH}_4\text{F}$  is raised.

### 3.2. Stirred electrolyte

A set of the voltage–time curves for anodizing aluminium at  $10 \text{ mA cm}^{-2}$  in the stirred FC electrolyte of variable concentrations in  $\text{NH}_4\text{F}$  is shown in Fig. 1(b) and compared with the voltage–time curve in the stirred FF working solution. From comparison of Figs. 1(a) and (b), stirring of the FF working solution results in increase in the steady-state voltage. Conversely, the presence of fluoride species in the working solution makes anodizing behaviour of aluminium significantly different from that in the FF oxalic acid solution. First, the value of anodizing voltage decreases from 50 to 3 V, more noticeably than in the non-stirred FC electrolyte. With the addition of relatively low amounts of ammonium fluoride, after reaching a maximum value ( $E_{\text{cr}}$ ) the voltage scarcely changes during the anodizing period (curves 2–3). With the further increase in  $C_{\text{F}}$ , after reaching  $E_{\text{cr}}$  the voltage continues to rise almost linearly, although at a substantially reduced rate (curves 4–8), with a slope  $dE/dt$ , which becomes larger, reaching a maximum of  $0.25 \text{ V min}^{-1}$  (curve 5), and then lowers back to zero. Eventually, at a concentration of  $2.5 \text{ mmol dm}^{-3}$ , the anodizing voltage decreases to a minimal value of 3 V.

### 3.3. Voltage–concentration behaviour

Fig. 2 summarizes the data obtained from studying the voltage–time response for anodizing of aluminium in the stirred and non-stirred electrolytes employed here. In the figure,  $E_{\text{cr}} = f(C_{\text{F}})$  and  $E_{\text{cur}} = f(C_{\text{F}})$  in the non-stirred FC electrolyte and  $E_{\text{cr}} = f(C_{\text{F}})$  in the stirred FC electrolyte are displayed. In the non-stirred electrolyte before  $C_{\text{F}} = 1.6\text{--}2.0 \text{ mmol dm}^{-3}$ ,  $E_{\text{cr}}$  exceeds  $E_{\text{cur}}$ , but thereafter the inverse situation occurs. An interesting feature is that, after  $1.2\text{--}1.6 \text{ mmol dm}^{-3}$  and contrary to the main trend, both the voltages exhibit a distinctive rise. Around this concentration region, the experiment was repeated three times and the phenomenon was

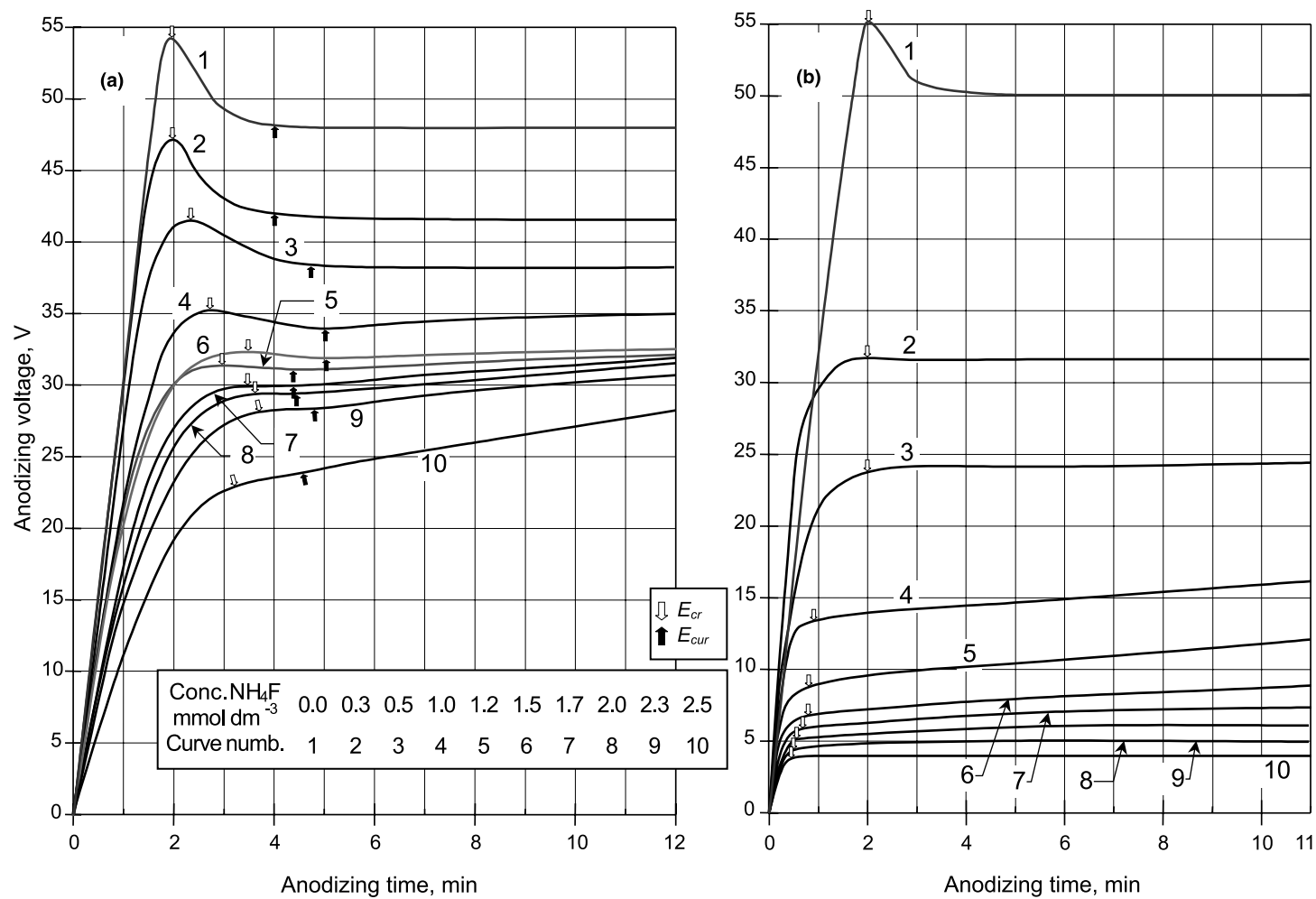


Fig. 1. Voltage–time responses for anodizing aluminium at a constant current density of  $10 \text{ mA cm}^{-2}$  in aqueous  $0.4 \text{ mol dm}^{-3} \text{ H}_2\text{C}_2\text{O}_4$ -containing variable amount of  $\text{NH}_4\text{F}$ : (a) stirring off, (b) stirring in.

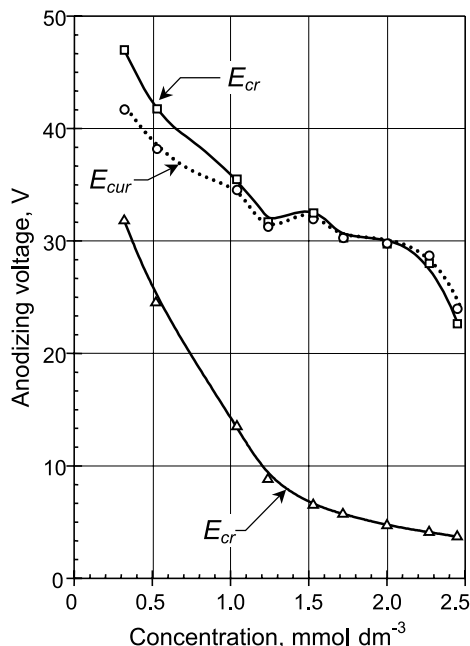


Fig. 2. Variation of anodizing voltage ( $E_{cr}$  and  $E_{cur}$  as pointed out in Fig. 1) with concentration of ammonium fluoride in aqueous  $0.4 \text{ mol dm}^{-3} \text{ H}_2\text{C}_2\text{O}_4$ . Anodizing of aluminium was performed at a constant current density of  $10 \text{ mA cm}^{-2}$ : (a) stirring off, (b) stirring in.

definitely confirmed. It is also seen that, in the stirred FC electrolyte after  $C_F = 1.4 \text{ mmol dm}^{-3}$ ,  $E_{cr}$  continues to decrease, but at a substantially reduced rate. Thus,  $C_F$  value of around  $1.4 \text{ mmol dm}^{-3}$  seems to be a critical concentration affecting the voltage–time behaviour for anodizing aluminium in the FC electrolytes employed in this study.

It was shown in our previous work [12] that galvanostatic anodizing of aluminium in oxalic acid solutions proceeds at 96% Faradaic efficiency, independently of electrolyte concentration and anodic current density. According to [12], the rate of anodizing aluminium metal,  $V_a$ , is given by

$$V_a (\text{cm s}^{-1}) = Ai (\text{mA cm}^{-2}), \quad (1)$$

in which  $i$  is the anodic current density,  $A$  is the coefficient that depends on the current efficiency and is equal to  $3.33 \times 10^{-8} \text{ cm s}^{-1} \text{ mA}^{-1}$  for anodizing aluminium in pure oxalic acid electrolytes [12]. In the present work, to assess the current efficiency for anodizing in the FC electrolytes the initially deposited aluminium films, of essentially the same thicknesses, were fully oxidized in all the electrolytes employed up to the oxide-coated Si substrates and then the anodizing rates were compared to estimate the value of  $A$  in Eq. (1) for each electrolyte. It appeared that the anodizing rate in the non-stirred FC electrolytes is practically the same as that in the FF working solution, which implies the same value of  $A$  and hence, the same current efficiency of 96%. However, in

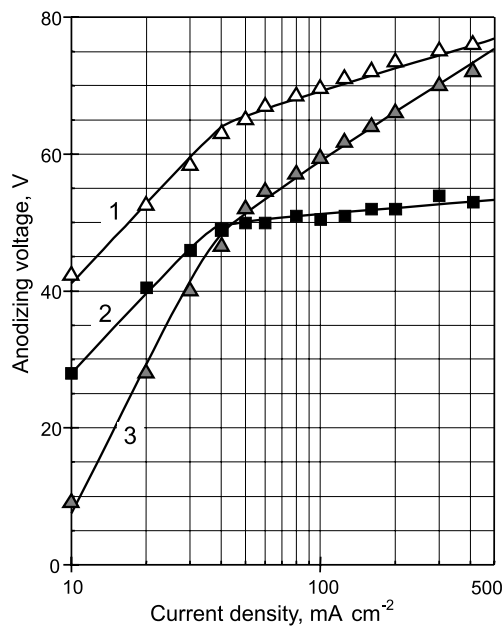


Fig. 3. Variation of anodizing voltage with current density for (1) steady-state aluminium anodizing in non-stirred  $0.4 \text{ mol dm}^{-3} \text{ H}_2\text{C}_2\text{O}_4$ , (2) for anodizing in non-stirred  $1.4 \text{ mmol dm}^{-3} \text{ NH}_4\text{F}$ ,  $0.4 \text{ mol dm}^{-3} \text{ H}_2\text{C}_2\text{O}_4$ , and (3) for anodizing in stirred  $1.4 \text{ mmol dm}^{-3} \text{ NH}_4\text{F}$ ,  $0.4 \text{ mol dm}^{-3} \text{ H}_2\text{C}_2\text{O}_4$ .

the stirred FC electrolyte the anodizing rate was found to be relatively higher and  $A$  value was estimated to be  $3.45 \times 10^{-8} \text{ cm s}^{-1} \text{ mA}^{-1}$ . This indicates that anodic oxidation in the stirred FC electrolytes proceeds without any by-process at the Faradaic efficiency approaching 100% [12].

### 3.4. Voltage–current behaviour

Variations of  $E_{cr}$  value with current density of galvanostatic anodizing aluminium in the stirred and non-stirred working solutions modified by a constant amount of  $\text{NH}_4\text{F}$  are shown in Fig. 3 and compared with the steady-state voltage–current curve for anodizing aluminium in the non-stirred FF working solution over the same current range. In Fig. 3, two characteristic stages can be distinguished with a critical current density,  $i_{cr}$ , of about  $40 \text{ mA cm}^{-2}$ . Before and beyond  $i_{cr}$ , the experimental data can be linearly approximated, which implies the logarithmic character of the curves. An interesting feature in the stirred FC electrolyte is that, being relatively much lower at the initial current densities, the anodizing voltage then rises at a relatively higher rate and beyond  $i_{cr}$  begins to progressively exceed the voltage taking up in the non-stirred FC electrolyte. Finally, at the very high current density the voltage in the stirred FC electrolyte closely approaches the steady-state voltage in the FF working solution.

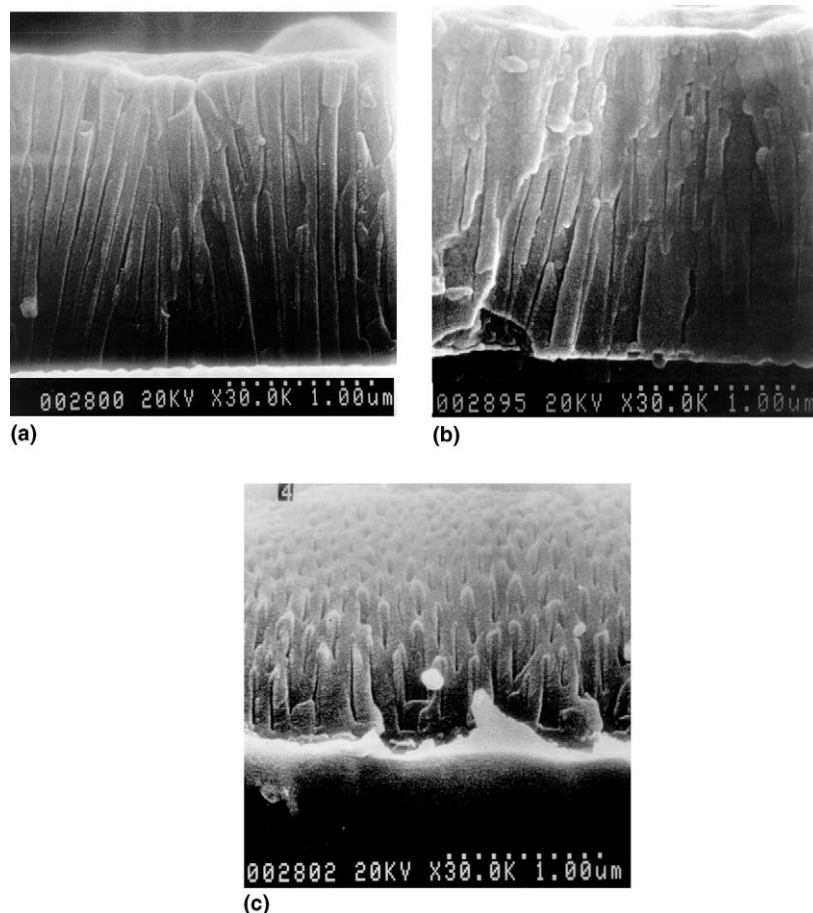


Fig. 4. Scanning electron micrographs of fracture-sections of porous oxide films formed by galvanostatic anodizing at  $10 \text{ mA cm}^{-2}$  for 7 min in (a)  $0.4 \text{ mol dm}^{-3} \text{ H}_2\text{C}_2\text{O}_4$  at 50 V, (b) non-stirred  $0.5 \text{ mmol dm}^{-3} \text{ NH}_4\text{F}$ ,  $0.4 \text{ mol dm}^{-3} \text{ H}_2\text{C}_2\text{O}_4$  at 38 V and (c) stirred  $2.5 \text{ mmol dm}^{-3} \text{ NH}_4\text{F}$ ,  $0.4 \text{ mol dm}^{-3} \text{ H}_2\text{C}_2\text{O}_4$  at 3 V.

### 3.5. Structural parameters

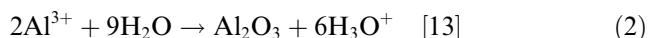
SEM photographs of fracture-sections of alumina films formed at a constant current density of  $10 \text{ mA cm}^{-2}$  for 7 min in the stirred FC electrolytes of an average concentration and a maximum concentration of  $\text{NH}_4\text{F}$  are shown in Figs. 4(b) and (c), and compared with SEM photograph of a local region of a film grown in the FF working solution at the same anodizing conditions (Fig. 4(a)). Of the three specimens, no much difference in the porous-cellular structures is observed in the photographs: the mean diameter of alumina oxide cells and the thickness of oxide barrier layer can be estimated as 130 and 60 nm, respectively.

## 4. Discussion

Possible explanation of the behaviour determined is based on the following assumptions.

(1) It is most probable that fluorine species are present in the electrolyte in the form of uncharged HF

molecules, which result from the reaction of  $\text{F}^-$  ions from  $\text{NH}_4\text{F}$  dissociating with (i) hydrogen ions derived from  $\text{H}_2\text{C}_2\text{O}_4$  dissociating or (ii) hydrogen ions generated at the film surface as a by-product of film growth by the reactions



Reaction (3) seems very possible since dissociation constant for HF is very low ( $6.6 \times 10^{-4}$ ) and is about hundredfold lower than that for  $\text{H}_2\text{C}_2\text{O}_4$  ( $5.6 \times 10^{-2}$ ). Thus,  $\text{F}^-$  ions derived from ammonium fluoride molecules are scarcely present in the bulk electrolyte and practically are not involved in charge transfer in the electrolyte.

(2)  $\text{Al}^{3+}$  ions dissolved from growing oxide and  $\text{Al}^{3+}$  ions direct-ejected to the electrolyte [14,15] react with neutral HF molecules in the bulk electrolyte to produce stable negatively charged fluoride complexes of aluminium, which are presumed to be incorporated into growing oxide. The generalized form of the reaction is



The incorporation of such species into the barrier layer comprises transport of  $[\text{AlF}_n]^{(n-3)-}$  complexes from the bulk electrolyte along the pores into, and then across, the diffusion layer to the barrier layer/electrolyte interface, adsorption of the complexes on the pore bases and finally direct incorporation of the absorbed complexes into, and migration inwards in, the barrier layer. The last step may be more complex and can involve a transformation of the absorbed complex to a new form of anion [13].

It is believed that the complex process of incorporation of electrolyte-derived species, including FC ones, into the barrier layer should not be explained only by a simple size effect. Bogoyavlenskii [16] has suggested that, during porous alumina growth, the barrier layer is activated into a state in which the ions act like colloid particles under the high electric field and at elevated temperatures at the pore bases. This assumption correlates with a 'liquid' droplet model suggested more recently by Mott [17] and supported by Shimizu et al. [18]. Belov [19] has also suggested a model in which oxide barrier layer, being considerably ionic in nature, is described as a solid electrolyte during oxide formation. In both cases the models imply migration inwards of negatively charged electrolyte-derived species of bigger sizes than  $\text{O}^{2-}$ ,  $\text{OH}^-$  or even  $\text{PO}_4^{3-}$ ,  $\text{SO}_4^{2-}$ , and  $\text{C}_2\text{O}_4^{2-}$ . Possible incorporation of  $\text{HC}_2\text{O}_4^-$ ,  $\text{H}_2\text{PO}_4^-$ ,  $\text{HPO}_4^{2-}$  anions, aluminium oxalate-complexes and aluminium phosphate-complexes into porous alumina film has also been stated in our previous works and discussed by some other authors [12,14,20,21]. Additionally, singly charged  $\text{F}^-$  ions of ionic radius almost equal to that of  $\text{O}^{2-}$  ions (0.132 and 0.133 nm, respectively) are also expected to be incorporated into the growing oxide as the original ions competitively with doubly charged oxygen anions [18,22]. The presence of singly charged fluoride ions in the diffusion layer can be explained as being due to HF molecule dissociation under the high electric field to give  $\text{F}^-$  ions, which are then absorbed on the pore bases. However, both the fluoride ions and the FC species are presumed to derive chiefly from neutral HF molecules, which are present in the bulk electrolyte and need to be transported to the film/electrolyte interface.

From Fig. 1(a), the addition of ammonium fluoride lowers the voltage taken up during galvanostatic aluminium oxidation. Similarly to this and contrary to the situation with the FF working solution (Fig. 1(b)), stirring of the FC electrolyte appeared to cause the additional and significant decrease in the forming voltage. As the changes described are suggested to result from the presence of HF in the electrolyte, it should be noted that the neutral HF molecules could be transported to the film area only by means of diffusion. Obviously, the stirring intensively exchanges portions of the electrolyte

in the vicinity of the alumina surface and thus provides effective transport of HF molecules to the film surface. If this were not the case, the stirring would hardly ever produce such a strong effect on the voltage–time behaviour in the FC electrolyte.

From Figs. 1 and 2, the higher the concentration of ammonium fluoride in the electrolyte the lower the anodizing voltage. Similarly, this can be explained by increasing the amount of HF formed in the electrolyte with increasing the amount of  $\text{NH}_4\text{F}$  added to the working solution. Further, despite a lack of  $\text{F}^-$  ions present in the bulk electrolyte, concentration, for instance, of  $[\text{AlF}_6]^{3-}$  complex anion is expected to be comparable with, or even higher than, that of  $[\text{Al}(\text{C}_2\text{O}_4)_3]^{3-}$  complex anion because the insolubility of  $[\text{AlF}_6]^{3-}$  complex in aqueous media is relatively higher than that of  $[\text{Al}(\text{C}_2\text{O}_4)_3]^{3-}$  (stability constant is 20.67 and 16.3, respectively). Moreover, considering size difference of the both complexes, the mobility of the fluoride complex is likely to be relatively higher too. Thus, the increase in  $\text{NH}_4\text{F}$  concentration in the working solution leads to increase in a number of  $[\text{AlF}_6]^{3-}$  complexes, which move along the pores, enter the barrier layer and migrate inwards under the high field applied. As the geometrical parameters, including the barrier layer thickness, of films formed at the substantially different voltages do not exhibit visible changes (Fig. 4), it implies that the ionic resistivity of the barrier layer becomes significantly lower in the FC electrolyte, due to the presence of incorporated fluoride species. Alternatively, it is possible that ionic conduction through the overall electrochemical circuit 'diffusion layer–double layer–oxide barrier layer' becomes easier, owing to a series of processes involved in transport of mobile fluoride complexes into the diffusion layer, specific sorption of the complexes on the pore bases, and incorporation of the complexes into the growing oxide.

The changes in the voltage–time responses at the commencement of anodizing (see Fig. 1(a)) can be explained by possible reorganization of self-nucleation and initial growth of alumina cells and pores. As the initial 'stoop' at the voltage–time curves gradually flattens and eventually disappears with increasing concentration of FC species in the electrolyte, it is very probable that the pore mouth becomes relatively wider, but the changes may be too small to be determined precisely by SEM at the available resolution.

The gradual voltage rise after  $E_{\text{cur}}$  in the non-stirred FC electrolyte and the increase in  $dE/dt$  with increasing  $\text{NH}_4\text{F}$  concentration (see Fig. 1(a)) can be explained by considering that the transport of HF molecules along growing and such a narrow pore to the pore base becomes more and more obstructed while the pore length increases. As the amount of HF that is needed to maintain the voltage at its 'abnormally' low level becomes insufficient, the voltage begins to rise intending to

compensate the deficiency of HF inside the pore and to reach its adequate value. Importantly, as this phenomenon affects the ionic resistivity of growing barrier layer but not the structural parameters of porous film, it allows consideration of this period of alumina formation as the steady-state oxide growth [10].

The slope  $dE/dt$  for films grown in the stirred FC electrolyte at medium  $\text{NH}_4\text{F}$  concentrations (see Fig. 1(b)) has probably the same origin as that in the non-stirred FC electrolyte, but the slope eventually becomes negligible (curves 9–10) due to transporting a sufficient amount of HF to the film surface and due to pore widening at the film surface followed by partial dissolution of the upper part of film, owing to increasing aggressiveness of the electrolyte [23].

It is known that, when anodizing current is raised, especially above  $10 \text{ mA cm}^{-2}$ , the temperature of electrolyte inside alumina pores and at the film/electrolyte interface increases rapidly causing a decrease in forming voltage [20]. Here from Fig. 3, for the non-stirred FC electrolyte, the elevation of the forming voltage retards substantially beyond  $45 \text{ mA cm}^{-2}$ , which can be similarly explained by local overheating of the oxide/electrolyte interface. On the other hand, the rate of voltage rise for anodizing in the stirred FC electrolyte is obviously greater than that in the non-stirred FC electrolyte. It can be concluded that, under the elevated temperatures, the stirring provides an effective cooling of the film/electrolyte interface in the FC electrolyte, which probably contributes more essentially to the voltage rise than the relevant increase in HF concentration at the alumina surface contributes to the corresponding voltage drop.

## 5. Conclusion

The voltage–time behaviour for galvanostatic anodizing of aluminium in the stirred and non-stirred  $0.4 \text{ mol dm}^{-3}$  oxalic acid electrolytes modified by variable amount of ammonium fluoride, in a wide range of current densities was studied, with several important features emerging.

1. Anodizing in the FC electrolyte proceeds at a relatively lower voltage compared with the FF oxalic acid solution but at the same Faradaic efficiency of 96%.
2. Stirring of the FC electrolyte increases the Faradaic efficiency up to 100%, enhances substantially the voltage-reducing effect, resulting in lowering the steady-state voltage to a value of 3 V at a sufficiently high current density of  $10 \text{ mA cm}^{-2}$ .
3. Despite the significant differences in the forming voltages depending on  $\text{NH}_4\text{F}$  concentration, no apparent changes in pore morphologies of the films and in the

barrier layer thickness are revealed from SEM observations.

4. The behaviour determined is reasonably explained by considering formation, transport to the diffusion layer, specific sorption and further incorporation into the barrier layer of FC species derived from reaction of  $\text{Al}^{3+}$  ions with the electrolyte elements.

In conclusion, further detailed analysis of the element composition of the films formed in FC acidic electrolytes, the structural parameters and dielectric properties of the films are expected in future works.

## References

- [1] G.C. Schwartz, V. Platter, *J. Electrochem. Soc.* 122 (1975) 1508.
- [2] G.C. Schwartz, V. Platter, *J. Electrochem. Soc.* 123 (1976) 34.
- [3] V. Sarganov, A. Mozalev, *Zarubezhnaya Elektronnaya Tekhnika* 1–2 (1993) 40.
- [4] V. Sarganov, *IEEE Trans. Components Pack. Manuf. Technol. B* 17 (1994) 197.
- [5] A. Mozalev, A. Sarganov, S. Magaino, *Electrochim. Acta* 44 (1999) 3891.
- [6] L. Young, *Anodic Oxide Films*, Academic Press, New York, 1960.
- [7] V. Sarganov, A. Mozalev, *Microelectron. Eng.* 37–38 (1997) 329.
- [8] Y. Shacham-Diamand, S. Lopatin, *Electrochim. Acta* 44 (1999) 3639.
- [9] H. Masuda, F. Hasegawa, S. Ono, *J. Electrochem. Soc.* 144 (1997) L127.
- [10] J.P. O'Sullivan, G.C. Wood, *Proc. R. Soc. Lond. A* 317 (1970) 511.
- [11] V. Sarganov, G. Gorokh, A. Mozalev, A. Poznyak, *Prot. Met. (Transl. Zashita Metallov)* 27 (1991) 125.
- [12] V. Sarganov, A. Mozalev, I. Mozaleva, *J. Appl. Chem. (Transl. Zh. Prikl. Khim.)* 68 (1995) 1638.
- [13] P. Skeldon, K. Shimizu, G.E. Thompson, G.C. Wood, *Philos. Mag. B* 72 (1995) 391.
- [14] M. Nagayama, H. Takahashi, in: R.W. Staehle (Ed.), *Proceedings of Passivity and Breakdown of Iron Base Alloys, USA–Jpn Seminar 1975*, Natl. Assoc. Corros. Eng., Houston, TX, 1976, p. 56.
- [15] M. Nagayama, K. Tamura, H. Takahashi, in: N. Sato (Ed.), *Proc. Intern. Cong. Metal Corrosion, Natl. Assoc. Corros. Eng., Houston, TX, 1974*, p. 175.
- [16] A.F. Bogoyavlenskii, in: A.F. Bogoyavlenskii (Ed.), *Proceedings of the 2nd Interuniversity Conference on 'Anode-68'*, USSR, Kazan, 1968, p. 3.
- [17] N.F. Mott, *Philos. Mag. B* 55 (1987) 117.
- [18] K. Shimizu, K. Kobayashi, G.E. Thompson, P. Skeldon, G.C. Wood, *Philos. Mag. B* 73 (1996) 461.
- [19] V.T. Belov, in: V. Belov (Ed.), *Proceedings of National R&D Conference on 'Anode-90'*, USSR, Kazan, 1990, p. 124 (Chapter 2).
- [20] V. Sarganov, A. Mozalev, I. Mozaleva, *J. Appl. Chem. (Transl. Zh. Prikl. Khim.)* 70 (1997) 267.
- [21] L.L. Odynets, *J. Appl. Chem. (Transl. Zh. Prikl. Khim.)* 65 (1992) 2417.
- [22] K. Shimizu, K. Kobayashi, P. Skeldon, G.E. Thompson, G.C. Wood, *J. Electrochem. Soc.* 144 (1997) 418.
- [23] J.W. Diggle, *Electrochim. Acta* 18 (1973) 283.